

CrystEngComm

Accepted Manuscript



This is an *Accepted Manuscript*, which has been through the Royal Society of Chemistry peer review process and has been accepted for publication.

Accepted Manuscripts are published online shortly after acceptance, before technical editing, formatting and proof reading. Using this free service, authors can make their results available to the community, in citable form, before we publish the edited article. We will replace this *Accepted Manuscript* with the edited and formatted *Advance Article* as soon as it is available.

You can find more information about *Accepted Manuscripts* in the [Information for Authors](#).

Please note that technical editing may introduce minor changes to the text and/or graphics, which may alter content. The journal's standard [Terms & Conditions](#) and the [Ethical guidelines](#) still apply. In no event shall the Royal Society of Chemistry be held responsible for any errors or omissions in this *Accepted Manuscript* or any consequences arising from the use of any information it contains.



Self-generated micro-cracks in an ultra-thin AlN/GaN superlattice interlayer and their influences on the GaN epilayer grown on Si(110) substrates by metalorganic chemical vapor deposition

Received 00th January 20xx,
Accepted 00th January 20xx

DOI: 10.1039/x0xx00000x

www.rsc.org/

Xu-Qiang Shen, Tokio Takahashi, Hirofumi Matsuhata, Toshihide Ide and Mitsuaki Shimizu

We investigate the effect of an ultra-thin AlN/GaN superlattice interlayer (SL IL) on the GaN epilayer grown on Si(110) substrates by metalorganic chemical vapor deposition (MOCVD). It is found that micro-cracks (MCs) are self-generated in the SL IL region, which depend on the thickness of the SL IL. The MCs influences the characteristics of the GaN epilayers grown on the SL IL, such as surface morphologies, strain and structural qualities. Furthermore, different MCs configurations depending on the SL IL thickness are observed, which imply the controllability of the MCs generation. The mechanism understanding and the optimization of the SL IL structure make it possible to grow crack-free high-quality GaN films on Si substrates for optic and electronic device applications.

1 Introduction

Recently, heteroepitaxial growth of high-quality III-nitrides on Si substrates is attracting a great attention due to its low-cost, large size availability and suitability in integration with Si electronics. However, large mismatches both in the lattice constant and the coefficient of thermal expansion (CTE) between GaN and Si^{1, 2} prevent from obtaining high-quality and crack-free thick GaN films grown on Si substrates. To overcome the crack problem, relaxation structures trying to compensate the CTE-induced tensile strain during the cooling down process after the growth have been proposed and the crack-free thick GaN and the device operations grown on Si substrates have been demonstrated.³⁻¹⁸

Among the proposed relaxation structures, an ultra-thin AlN/GaN superlattice interlayer (SL IL) structure shows a unique feature because it makes use of the naturally generated micro-crack (MC) during the cooling down process in the SL IL to compensate the CTE-induced tensile strain in the plasma-assisted molecular beam epitaxy (rf-MBE).^{18,19} As a result, a crack-free 4 μm thick continuous GaN epilayer grown on a Si(110) substrate has been realized by rf-MBE.²⁰ We have applied the technique to the growth of GaN epilayer on 4-inch Si(110) substrates by metalorganic chemical vapor deposition (MOCVD) because MOCVD technique is showed to be the best one for high-quality III-nitride film growth and mass production at present. A 2 μm thick continuous crack-free GaN film has been obtained using such an ultra-thin AlN/GaN SL IL structure.²¹ Furthermore, the optimized average Al

composition of the SL IL (treated as a quasi-AlGa_xN²²) is around 0.45 by totally taking account of both the strain and the wafer bowing issues. Since the growth conditions are completely different between the MOCVD and the rf-MBE growth, there are many unknown factors concerning the SL IL roles in the MOCVD-grown GaN on Si substrates, such as SL IL thickness effect on the strain modulation and the MC generation. Therefore, it is necessary to make them clear in order to control the growth and to obtain high-quality crack-free GaN films on Si substrates for optic and electronic device applications.

In this paper, we report the experimental results concerning the effect of an ultra-thin AlN/GaN SL IL on the GaN epilayer grown on Si(110) substrates by MOCVD. As a result, self-generated MCs in the SL IL region are observed, which depend on the thickness of the SL IL. The different MCs configurations influence the surface morphology, the residual tensile strain and the quality of the GaN epilayers grown on the SL IL, and can be controlled by the SL IL thickness.

2 Experimental

The samples were grown by MOCVD on 4-inch Si(110) substrates. Trimethylaluminum (TMA) and trimethylgallium (TMG) were used as III-group precursors for the growth of AlN and GaN. The growth temperature was set at 1070°C, and the growth chamber pressure during the growth and the cooling down process was kept at 30kPa. After the growth, the sample temperature was naturally reduced at a cooling rate of approximately 100 degree/minute under the mixed gases (NH₃+H₂+N₂) environment. The sample structure is described as following. After a ~100 nm AlN seed layer and a ~200 nm GaN buffer layer growth, an ultra-thin AlN(~1.8 nm)/GaN(~2.2 nm) SL IL was grown. Following, a ~2.0 μm GaN epilayer was

Advanced Power Electronics Research Center, National Institute of Advanced Industrial Science and Technology (AIST), Umezono 1-1-1, Central 2, Tsukuba-shi, Ibaraki, 305-8568, Japan. E-mail address: xq-shen@aist.go.jp

grown on the SL IL. To study the thickness effect of the SL IL, three samples were grown with the period of SL being 20, 40 and 60, respectively. *In-situ* wafer curvature measurements (LAYTEC EpiCurve[®]TT with a laser wavelength of 670 nm) were carried out to monitor the wafer curvature variation during the growth. This can help us to understand the details of the strain transition between each layer during the growth. Optical microscope (OM) and scanning transmission electron microscope (STEM) were used to observe the GaN surface morphology and the microstructures in the film. In addition, high-resolution X-ray diffraction (HRXRD) was used to characterize the residual strain and the structural quality of the GaN epilayers.

3 Results and discussion

Figure 1 shows the *in-situ* wafer curvature monitoring results of the three samples during the growth and the cooling down process. Due to the lattice constant mismatch, the wafer curvature experiences several changes during the different growth stages. Basically, the wafer curvature tends to develop to a convex shape during the GaN growth on AlN and SL IL, while those of AlN on Si and AlN/GaN SL IL on GaN change to a concave shape. Several results can be obtained from Fig. 1. First of all, the concave curvature during the SL IL growth on the GaN buffer layer increases with the increase of the SL IL period (SL IL thickness). Since the ultra-thin AlN/GaN SL can be treated as a quasi-AlGa_N layer, the equivalent tensile stress accumulated in the SL IL increases with the layer thickness.²³ However, the concave curvature of a 60-periods SL IL does not follow the trace as those of 20- and 40-periods samples at the latter half growth, which implies a structure change during the

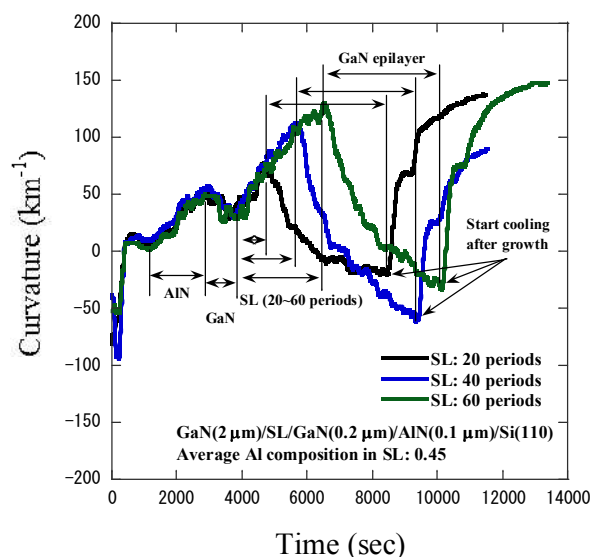


Fig. 1 *In-situ* wafer curvature monitoring results of the three samples with different AlN/GaN SL IL thicknesses during the growth by LAYTEC EpiCurve[®]TT with a laser wavelength of 670 nm.

SL IL growth as will be described later. The next feature is the compressive effect of the SL IL on the GaN epilayer grown on it. The curvature of the GaN epilayer changes to the convex direction due to the difference of the equivalent lattice constant between the quasi-AlGa_N and the GaN. From the absolute curvature change in the GaN epilayer growth, it is clear that the strongest compressive effect on the GaN epilayer is supplied by a 40-periods AlN/GaN SL IL, while the weakest one is by a 20-periods SL IL. The final phenomenon is the wafer curvature after cooling down to the room temperature (RT). The sample with a 40-periods AlN/GaN SL IL shows the smallest concave curvature, which means that this SL IL structure is the most effective one to compensate the

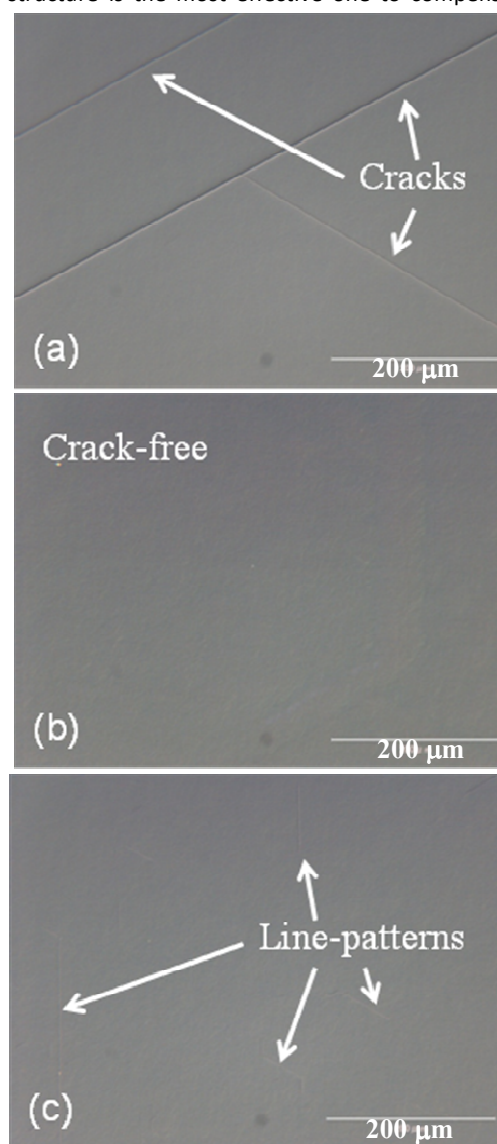


Fig. 2 Optical microscope (OM) images of three $\sim 2.0 \mu\text{m}$ thick GaN epilayers grown on the Si(110) substrates with different AlN/GaN SL IL thicknesses. The periods (thickness) of the SL IL are (a) 20 ($\sim 80 \text{ nm}$), (b) 40 ($\sim 160 \text{ nm}$) and (c) 60 ($\sim 240 \text{ nm}$), respectively. Large cracks are observed only from the sample (a).

CTE-induced tensile strain during the cooling down process. The above *in-situ* curvature monitoring results indicate that the ultra-thin AlN/GaN SL IL thickness plays an important role in the strain modulation during the GaN epilayer growth and the cooling down processes.

The surface morphologies of all samples are characterized by OM as shown in Fig. 2. Large cracks are unexpectedly observed from the sample with a 20-periods AlN/GaN SL IL (Fig. 2 (a)). The crack line is along the $\langle 11\text{-}20 \rangle$ direction. There are complete no small cracks between the large cracks. This kind of crack is believed to be generated during the cooling down process as discussed later. The sample with a 40-periods AlN/GaN SL IL shows a crack-free surface (Fig. 2 (b)), which corresponds to the smallest final wafer curvature at RT as shown in Fig. 1. On the other hand, the sample with a 60-periods AlN/GaN SL IL illustrates some small line-like patterns as marked by arrows (Fig. 2 (c)), which run in the same direction as those shown in Fig 2(a). These patterns are not cracks as those in Fig. 2 (a), but they seem to get a great influence from the beneath structure imperfection. In order to fully understand the above phenomena, it is necessary to carefully study the microstructures in the samples.

To investigate the origins of the above phenomena, cross-sectional STEM observations are carried out in the $\langle 11\text{-}20 \rangle$ direction of GaN, which is along the lateral crack propagating direction. Figure 3 shows the cross-sectional dark-field (DF) STEM images of the three samples together with the insets of the magnified high angle annular dark field (HAADF) images. Unique microstructures from the samples are observed, which can help us to understand the thickness effect of the SL IL on the upper GaN epilayer growth. When the SL IL is thin (20 periods, ~ 80 nm), no MCs are found in the SL IL position. This can be considered that the thickness of the SL IL with 20 periods does not exceed the critical thickness for the MC generation during the growth.²³ Instead, a large crack is observed going through the whole film as shown in Fig. 3(a), which corresponds to the cracks observed by OM (Fig. 2(a)). This large crack is considered to be generated during the cooling down process because the STEM image shows that the crack starts from the top of the GaN epilayer surface without any buried GaN in it. On the other hand, when the period of a SL IL is 40 (~ 160 nm), a MC is observed locating at the SL IL position as shown in Fig. 3(b). This means that the SL thickness exceeds the critical value for the MC generation. No large cracks are observed in the upper GaN epilayer, which implies that the SL IL with the MC can compensate part of the CTE-induced tensile strain during the cooling down process resulting in the crack-free GaN on Si substrates. The MC is limited within the SL IL position, and it is buried by the GaN as clearly shown by the magnified HAADF image in Fig. 3 (b). Since the MC is small, the upper ~ 2.0 μm thick GaN epilayer can cover the MC-induced imperfection by lateral growth resulting in a flat crack-free GaN film as shown in Fig. 2(b). However, a MC generated in a 60 periods (~ 240 nm) SL IL shows a different MC configuration compared to that in a 40 periods one. The MC propagates downward and extends its region to the Si substrate as shown in Fig. 3(c). An empty hollow is visible in the MC region, although the upper part of

the MC is buried by the GaN as shown by the magnified HAADF image. This phenomenon can be ascribed to a strong release of a tensile strain during a thick SL IL growth with a high average Al composition (~ 0.45). The deep MC generation can reduce the degree of the wafer concave curvature during the

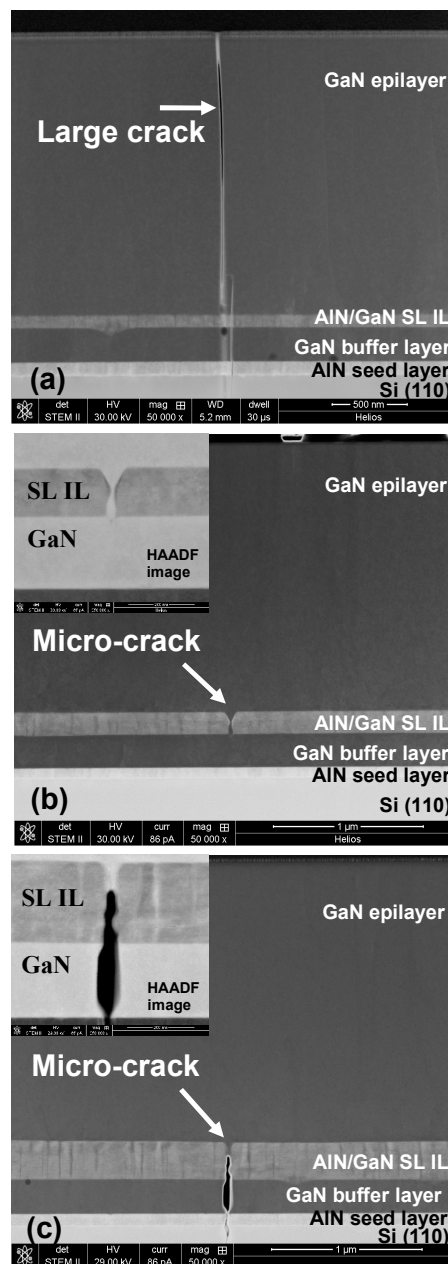


Fig. 3 Cross-sectional STEM images of three ~ 2.0 μm thick GaN epilayers grown on the Si(110) substrates with different AlN/GaN SL IL thicknesses. The periods (thickness) of the SL IL are (a) 20 (~ 80 nm), (b) 40 (~ 160 nm) and (c) 60 (~ 240 nm), respectively. MC can be found when the SL IL periods are 40 and 60, instead, a large crack going through the whole GaN is formed in the sample with a 20-periods SL IL. Insets are the magnified HAADF images clearly showing the different MC configurations with the buried GaN.

SL IL growth, which is reflected by the *in-situ* wafer curvature monitoring shown in Fig. 1. Furthermore, the large structure imperfection makes it difficult to completely flatten the surface by a ~ 2.0 μm thick GaN epilayer grown on it. That is why small line-like patterns are observed from a 60-periods SL IL sample surface as shown in Fig. 2(c). From the above results, it is estimated that the critical thickness for a MC generation in a SL IL with an average Al composition of 0.45 is between 80 and 160 nm and further detailed work is necessary to accurately determine it.

The different SL IL (treated as a quasi-AlGaIn) thicknesses greatly influence the compressive strain accumulation in the upper GaN epilayers during the growth.² When the SL IL is thin (20-periods), the compressive effect on the upper GaN epilayer is weak as shown in Fig. 1. Since there is no MC generation in the SL IL for an additional tensile strain compensation, a ~ 2.0 μm thick GaN epilayer (far over a critical thickness of ~ 0.3 μm for cracking) can not bear the CTE-induced tensile strain during the cooling down process resulting in a large crack formation as observed by OM and STEM. On the other hand, a thick SL IL (40 and 60 periods) can offer an enough compressive strain to the upper GaN epilayer as shown in Fig. 1. It can compensate the CTE-induced tensile strain by the compressive strain release together with the MC effect after the growth avoiding the large crack generation.²⁰ However, different MC configurations shown in Fig. 3 (b) and (c) do influence the compressive degree offered by the SL IL to the upper GaN epilayer. It is believed that the MC limited only in the SL IL position (in case of the 40-periods SL IL) can provide the strongest compressive strain to the upper GaN epilayer, which is supported by the *in-situ* curvature monitoring results. The final net residual strain in the upper GaN epilayer depends on the above discussed strain

compensation mechanism. Figure 4 shows the dependences of the net residual strain and the structural quality of the GaN epilayer on the SL IL thickness measured by HRXRD. All samples are in a tensile strain state, and the sample with a 40-periods SL IL shows the smallest tensile strain. The strain state is different from the results in rf-MBE-grown samples because the MC configuration and the MC generation mechanism are different between the two growth techniques.¹⁹ The structural quality of the GaN epilayer depends on the SL IL thickness as shown in Fig. 4, and the best values of the full width at half maximum (FWHM) of a 40-periods sample are 448 arcsec and 716 arcsec from the (002) and (102) diffraction peaks, respectively. From the above values, it is estimated that the screw and the edge dislocation densities in the GaN epilayer are $\sim 2.0 \times 10^8$ cm^{-2} and $\sim 1.3 \times 10^9$ cm^{-2} , respectively.²⁵

Based on the above experimental results and discussions, clear images of the AlN/GaN SL IL thickness effect on the MC generation and the strain modulation in the upper GaN epilayer are obtained. Ultra-thin AlN/GaN SL acting as a quasi-AlGaIn layer receives a tensile strain from the beneath GaN buffer layer and turns to a concave bending during the growth. When the SL IL thickness exceeds the critical value for cracking, the MC will be generated to relax the tensile strain.^{23,24} From the burying of GaN in the MC shown in Fig. 3, it is assumed that the MC is generated during the SL growth before the GaN epilayer growth. The cracking depends on the accumulation degree of the tensile strain in the SL IL, where the MC can limit within the SL IL region or propagate into the beneath GaN or even into the Si substrate with a large empty hollow structure. In addition, the different MC configurations influence the compressive effect of the SL IL on the upper GaN epilayer during the growth. Our experimental results show that the small MC terminating within the SL IL can provide the strongest compressive effect on the upper GaN epilayer during the growth. Furthermore, the small MC formation makes it easy to be buried by the upper GaN epilayer resulting in a crack-free GaN epilayer growth.

Conclusions

In conclusion, we investigate the effect of an ultra-thin AlN/GaN SL IL on the GaN epilayers grown on Si(110) substrates by MOCVD. It is found that the thickness of the SL IL plays an important role in the MC generation and results in the different MC configurations. The different MC configurations greatly influence the surface morphology, the residual tensile strain and the structural quality of the GaN epilayers grown on the SL IL. The estimated critical thickness for the MC generation in the SL IL with an average Al composition of 0.45 is between 80 and 160 nm. A complete crack-free 2.0 μm thick GaN epilayer grown on a Si(110) substrate with smooth surface and high structural qualities, is obtained by the use of a 40-periods SL IL. The mechanism understanding of the MC generation and the optimization of the SL IL structure make it possible to grow high-quality crack-free GaN films on Si substrates for optic and electronic device applications.

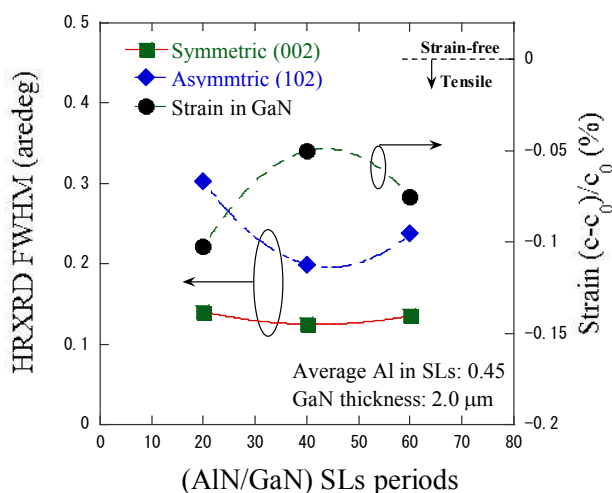


Fig. 4 Dependence of the residual tensile strain together with the FWHM values of (002) and (102) diffractions on the SL IL period from the ~ 2.0 μm thick GaN epilayers grown on Si(110) substrates measured by HRXRD. The sample with a 40-periods SL IL shows the smallest residual tensile strain and the best structural qualities.

Acknowledgements

Authors would like to thank H. Goto for the careful STEM sample preparations and observations.

Growth, 1990, **104**, 533.
25 P. Gay, P. B. Hirsch, and A. Kelly, *Acta Metall.* 1953, **1**, 315.

Notes and references

- 1 H. Ishikawa, G.Y. Zhao, N. Nakada, T. Egawa, T. Jimbo, and M. Umeno, *Jpn. J. Appl. Phys.* 1999, **38**, L492.
- 2 S. Raghavan and J.M. Redwing, *J. Appl. Phys.* 2005, **98**, 023514.
- 3 A. Able, W. Wegscheider, K. Engl, and J. Zweck, *J. Cryst. Growth*, 2005, **276**, 415.
- 4 S.L. Selvaraj, A. Watanabe, and T. Egawa, *Appl. Phys. Lett.* 2011, **98**, 252105.
- 5 W. Liu, J.J. Zhu, D.S. Jiang, and H. Yang, *Appl. Phys. Lett.* 2007, **90**, 011914.
- 6 K. Cheng, M. Leys, S. Degroote, M. Germain, and G. Borghs, *Appl. Phys. Lett.* 2008, **92**, 192111.
- 7 A. H. Blake, D. Caselli, C. Durot, J. Mueller, E. Parra, J. Gilgen, A. Boley, D.J. Smith, I.S.T. Tsong, J.C. Roberts, E. Piner, K. Linthicum, J.W. Cook, Jr., D. D. Koleske, M. H. Crawford, and A. J. Fischer, *J. Appl. Phys.* 2012, **111**, 033107.
- 8 L. Lu, Y.H. Zhu, Z.T. Chen, and T. Egawa, *J. Appl. Phys.* 2011, **109**, 113537.
- 9 E. Feltin, B. Beaumont, M. Laugt, P. de Mierry, P. Vennegues, H. Lahreche, M. Leroux, and P. Gibart, *Appl. Phys. Lett.* 2001, **79**, 3230.
- 10 E. Frayssinet, Y. Cordier, H. P. David Schenk, and A. Bavard, *Phys. Status Solidi* 2011, **C8**, 1479.
- 11 H.P.D. Schenk, E. Frayssinet, A. Bavard, D. Rondi, Y. Cordier, and M. Kennard, *J. Cryst. Growth*, 2011, **314**, 85.
- 12 A. Dadgar, F. Schulze, M. Wienecke, A. Gadanez, J. Blasing, P. Veit, T. Hempel, A. Diez, J. Christen, and A. Krost, *New J. Phys.* 2007, **9**, 389.
- 13 Y. Cordier, J.C. Moreno, N. Baron, E. Frayssinet, S. Chenot, B. Damilano, and F. Semond, *IEEE Electron Device Lett.* 2008, **29**, 1187.
- 14 B. Damilano, F. Natali, J. Brault, T. Huault, D. Lefebvre, R. Tauk, E. Frayssinet, J.C. Moreno, Y. Cordier, F. Semond, S. Chenot, and J. Massies, *Appl. Phys. Express*, 2008, **1**, 121101.
- 15 F. Reiher, A. Dadgar, J. Blasing, M. Wienecke, M. Muller, A. Franke, L. Reibmann, J. Christen, and A. Krost, *J. Phys D: Appl. Phys.* 2009, **42**, 055107.
- 16 F. Reiher, A. Dadgar, J. Blasing, M. Wienecke, and A. Krost, *J. Cryst. Growth*, 2010, **312**, 180.
- 17 Y. Cordier, J.C. Moreno, N. Baron, E. Frayssinet, J.M. Chauveau, M. Nemoz, S. Chenot, B. Damilano, and F. Semond, *J. Cryst. Growth*, 2010, **312**, 2683.
- 18 X.Q. Shen, T. Takahashi, H. Kawashima, T. Ide and M. Shimizu, *Appl. Phys. Lett.* 2012, **101**, 031912.
- 19 X. Q. Shen, T. Takahashi, X. Rong, G. Chen, X. Q. Wang, B. Shen, H. Matsuhata, T. Ide and M. Shimizu, *Appl. Phys. Lett.* 2013, **103**, 231908.
- 20 X.Q. Shen, T. Takahashi, H. Kawashima, T. Ide, M. Shimizu, and H. Okumura, *Jpn. J. Appl. Phys.* 2013, **52**, 08JB05.
- 21 X. Q. Shen, T. Takahashi, T. Ide, and M. Shimizu, *Phys. Status Solidi B*, 2015, **252**, 1075.
- 22 Y. Kawakami, A. Nakajima, X. Q. Shen, G. Piao, M. Shimizu, and H. Okumura, *Appl. Phys. Lett.* 2007, **90**, 242112.
- 23 S. Einfeldt, V. Kirchner, H. Heinke, M. Diebelberg, S. Figge, K. Vogeler, and D. Hommel, *J. Appl. Phys.* 2000, **88**, 7029.
- 24 K. Ito, K. Hiramatsu, H. Amano, and I. Akasaki, *J. Cryst.*